University of Baghdad
College of Engineering
JOURNAL OF ENGINEERING

Journal of Engineering

journal homepage: www.joe.uobaghdad.edu.iq

Volume 29 Number 12 December 2023

Numerical Simulation of Pile Group Response in Slope Layered Soil under the Effect of Seismic Loading

Mustafa A. Ismael[1,*], Balqees A. Ahmed[2]

[1]Department of Civil Engineering, Iraq University College, Basra, Iraq
[1,2]Department of Civil Engineering, College of Engineering, University of Baghdad, Baghdad-Iraq
mustafa.ismail2001m@coeng.uobaghdad.edu.iq[1], balqees.a@coeng.uobaghdad.edu.iq[2]

ABSTRACT

This work investigates the effect of earthquakes on the stability of a collective pile subjected to seismic loads in the soil layer. Plaxis 3D 2020 finite element software modeled pile behavior in dry soils with sloping layers. The results showed a remarkable fluctuation between the earthquakes, where the three earthquakes (Halabja, El Centro, and Kobe) and the acceleration peak in the Kobe earthquake had a time of about 11 seconds. Different settlement results were shown, as different values were recorded for the three types of earthquakes. Settlement ratios were increased by increasing the seismic intensity; hence the maximum settlement was observed with the model under the effect of the Kobe earthquake (0.58 g), where subsidence values at the three tremors differed between the pile distribution pattern. The highest drop recorded by the results was 60 mm in a distribution pattern 2×3. In general, increasing the size of the cap leads to an additional drop due to the weight of the cap.

Keywords: Slope, Pile group, Layer soil, Seismic load.

*Corresponding author
Peer review under the responsibility of University of Baghdad.
https://doi.org/10.31026/j.eng.2023.12.11

Article received: 14/02/2023
Article accepted: 17/08/2023
Article published: 01/12/2023

المحاكاة العددية لاستجابة مجموعة ركائز في التربة ذات الطبقات المنحدرة تحت تأثير الحمل الزلزالي

مصطفى احمد اسماعيل[1]*، بلقيس عبدالواحد احمد[2]

[1] قسم الهندسة المدنية، كلية العراق الجامعة، البصرة، العراق

[1،2] قسم الهندسة المدنية، كلية الهندسة، جامعة بغداد، بغداد، العراق

الخلاصة

في هذا العمل تم دراسة تأثير الزلازل على استقرار الركيزة الجماعية المعرضة لأحمال زلزالية في طبقة التربة. استخدم برنامج العناصر المحدودة (Plaxis 3D 2020) لنمذجة سلوك الركائز في التربة الجافة ذات الطبقات المنحدرة. وأظهرت النتائج تذبذبًا ملحوظًا بين الزلازل ، حيث الزلازل الثلاثة (حلبجة ، والسنترو ، وكوبي) واعلى ذروة تسارع كانت في زلزال كوبي في زمن امتد لحوالي 11 ثانية. عرضت نتائج الهبوط المختلفة ، حيث تم تسجيل قيم مختلفة للأنواع الثلاثة من الزلازل، وزادت نسب الهبوط بزيادة شدة الزلازل. ومن ثم لوحظ الحد الأقصى للهبوط مع النموذج تحت تأثير زلزال كوبي (0.58 غم) ، اختلفت قيم الهبوط عند الهزات الثلاثة بين نمط توزيع الركائز. كان أعلى انخفاض سجلته النتائج 60 ملم في نمط التوزيع 2 × 3. بشكل عام ، تؤدي زيادة حجم الغطاء إلى ازدياد إضافي في الهبوط بسبب وزن الغطاء.

الكلمات المفتاحية: ميل, مجموعة ركائز, تربة متطبقة, حمل زلزالي.

1. INTRODUCTION

There have been several severe slope collapses attributed to earthquakes in the past. Geotechnical engineering's estimation of the stability of slopes subject to seismic loads is a crucial problem. There are two useful estimating techniques for this issue. The first involves determining the slope's safety factor while considering pseudo-static earthquake body forces within a soil mass. **(Seed et al., 1969, Al-Taie, 2004, Al-Mosawe et al., 2007, Fattah et al., 2020)**. Because it is a simple extension of static considerations, the factor of safety notion has been frequently applied. It doesn't offer much information about the shaking procedure, though.

On the other hand, geotechnical engineers often use the technique of slopes stabilized by reinforcement to increase the stability of slopes. The stability of reinforced slopes for substantial earthquake acceleration may be overestimated using the pseudo-static method in engineering design **(Ling and Leshchinsky, 1998; Ling et al., 1965)**. The second one calculates the cumulative displacement exposed to seismic loads is computed in the second. The most typical strategy **(Newmark, 1965, Novak, 1974, Novak and Grigg, 1976 , Ben, 2013)** using the sliding block approach, which incorporates seismic acceleration into a single-block translational mechanism, slopes' cumulative displacement is calculated. This method has the benefit of being less time-consuming and of delivering information during an earthquake; it has also been expanded to include the rotating mechanism.

Because a weak layer's low shear strength impairs a slope's performance, weak layers in slopes demand specific consideration in engineering practice. Previous research on slopes with a weak layer was done in a static setting. **(Michalowski, 2007)** evaluated several approaches for determining the stability of a weak layer and nonhomogeneous soil slope. Additionally, finite element (FE) analysis combined with the shear strength reduction approach was used to examine the stability of a slope with a weak layer. **(Fredlund and Krahn, 1977; Griffiths and Marquez, 2007)**. Based on the upper-bound method, a rotational-translational collapse process was devised to evaluate the safety factor of slopes with a weak layer. The finite element technique was used to validate their analytical conclusions. However, little research has looked at how seismically resilient slopes with weak layers are. A weak or liquefied layer causes translational embankment failure, and the mechanics of such failure are demonstrated in **Fig. 1 (Ho, 2014).**

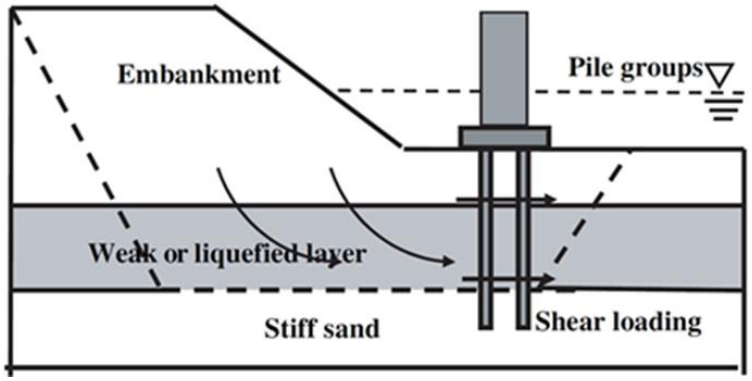

Figure 1. Shear loading acting on bridge piles is caused by lateral soil spreading **(Ho, 2014).**

This work assesses the stability of slopes with weak layers using a translational failure mechanism validated using an alternative static factor of safety solutions. A reinforced slope's critical yield acceleration coefficient is also calculated using a pseudo-static approach within the limit analysis framework. Finally, the cumulative displacement of two typical situations of slopes with a weak, thin layer is evaluated using Newmark's analytical technique using various genuine earthquake acceleration recordings as input motion. The main purpose of this study will be to ensure the significant performance of soil and single pile under different seismic loads in piles embedded in slope-layered soils and to generate useful parameters and required geotechnical data.

1.1 Piles in Slope Layer Soil

For many years, slope stabilization has involved the use of piles. Determining the shear pressures and bending moments created in the piles due to the movement of the unstable slope is one of the significant design difficulties. Although this type of slope stabilization has been used successfully (**Huang, 2013; Bowles, 1996; Reese et al., 2005; Shlash et al., 2012)**, there isn't a commonly agreed approach for the study and construction of these piles. It was derived previously by (**Ito and Matsui, 1975)** to evaluate the lateral force acting on a row of piles due to soil movement. Numerous failure modes of a stiff pile caused by the action of the sliding soil were hypothesized **(Fukuoka, 1977; Arosemena, 2007; Sowers,**

1996). As a result, group effects are not considered, and the approach is only relevant for piles at failure.

In this situation, slope instability leads to soil movements that create lateral stresses on the stabilizing piles interacting with one another. A consistent and logical analysis technique should thus consider all aspects of the soil-pile interaction issue.

For single piles, a simpler boundary element analysis approach is described **(Viggiani, 1981)**. The method relies on using Mindlin's solution to simulate the soil reaction, and it roughly accounts for the impact of non-homogeneous soil. The increasing ground inclination would generally increase spectral acceleration and excess pore pressure. When the ground inclination is higher enough, the kinematic force in the soil and the soil energy will dissipate more quickly. It would increase the pile's maximum lateral displacement and bending moment **(Lee, 1991)**.

1.2 Seismic Zones in Iraq

According to the Iraqi Seismic Code Requirements for Buildings (1997), for structural design, an evaluation of seismic hazards in various seismic zones should be put into practice based on the country's seismic zoning map. The relevant coefficients are displayed in **Fig. 2**.

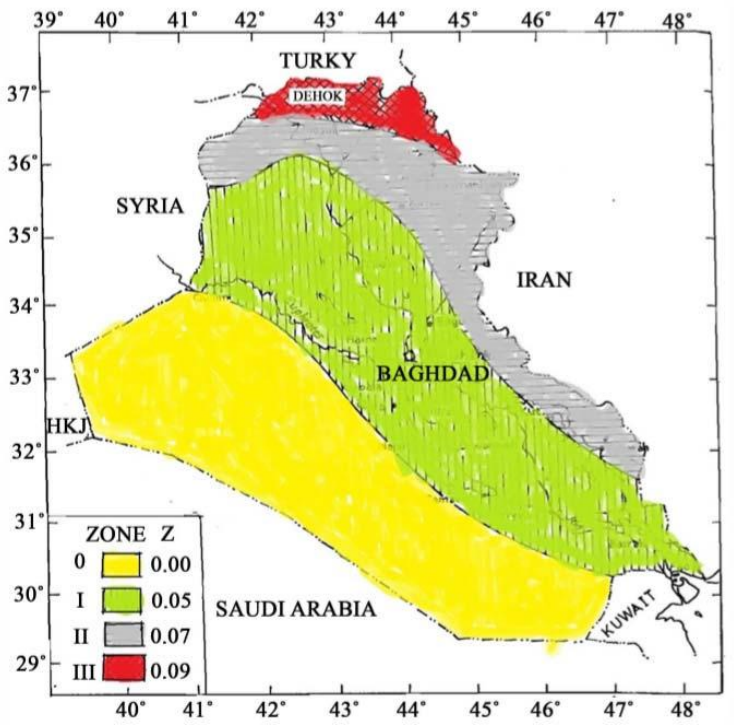

Figure 2. Seismic zone map of Iraq **(Amer et al., 2016)**

1.3 The Ultimate Failure Load

The failure loads are calculated using the load-settlement curves. Engineers generally agree that a failure load results in a settlement equal to 10% of the pile's diameter or width, as proposed in (**Terzaghi, 1943)**.

2. NUMERICAL SIMULATION

Conducting non-linear soil behavior is much easier thanks to the study's powerful analytical and numerical tools and the high-speed computer used in the analysis. One of the most productive strategies for finding geotechnical engineering solutions is the finite-element method (FEM). This has evolved into a significantly more successful strategy for overcoming geotechnical challenges. In this work, the finite element program Plaxis 3D 2020 is utilized to analyze the soil layers beneath a pile group positioned on a slope. The program was improved, primarily in stability, analytical deformation, and foundation projects. During this research, the Mohr-Coulomb standard was used to state soil conduct because it was a well-known model used as the first approach to soil conduct. This was done because the Mohr-Coulomb model was the initial method for soil conductivity. The model's name is a bilinear model. It is defined by four input parameters: the angle of internal friction (∅) calculated by Eq. (1) **(Hatanaka and Uchida, 1996)**, the elasticity modulus (E), and the Poisson's ratio (μ), and the cohesion (c), **(Albusoda, 2016)**.

$$\emptyset = \sqrt{20 \times N_{60}} + 20 \quad (1)$$

where:
∅ is the angle of internal friction, degree, and
N_{60} is SPT N-value corrected for field procedures only.

2.1 Simulation of Pile Material

This investigation's model has dimensions of (80m × 20m) and a thickness of 19.5 m. The pile was assumed to be a linear elastic body. The physical parameters were changed to ideal concrete values to make the foundation stiff, with a solid modulus E_c of 30 GPa, concrete unit weight of 25 kN/m^3, and Poisson's ratio of 0.15. The scenario is depicted in **Fig. 3,** along with its geometrical organization.

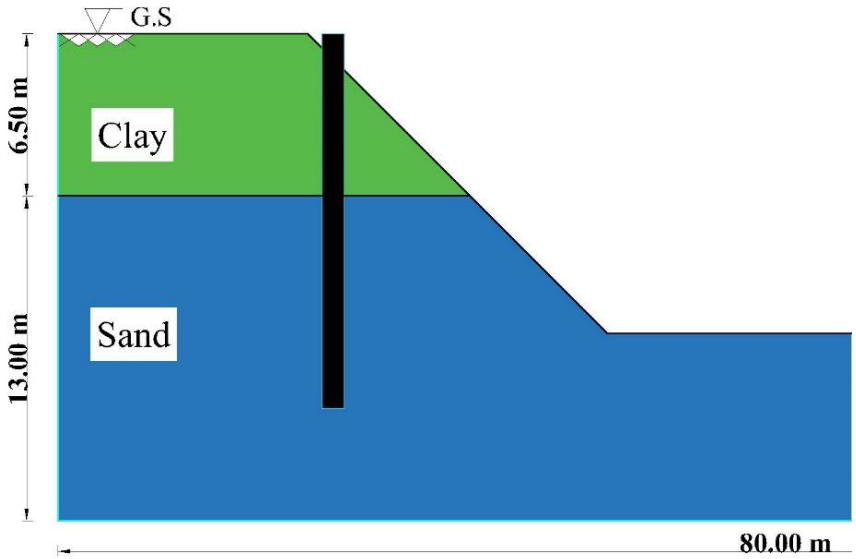

Figure 3. The situation's geometrical layout.

2.2 Pile Model

The concrete pile model utilized in this work has the parameters presented in **Table 1.**

Table 1. Pattern and characteristics of the employed concrete pile.

Diameter (m)	Length (m)	A pattern pile group	Spacing between the piles (center to center) (s), m
0.75	15	2×1	1.5
		2×2	1.5
		2×3	1.5

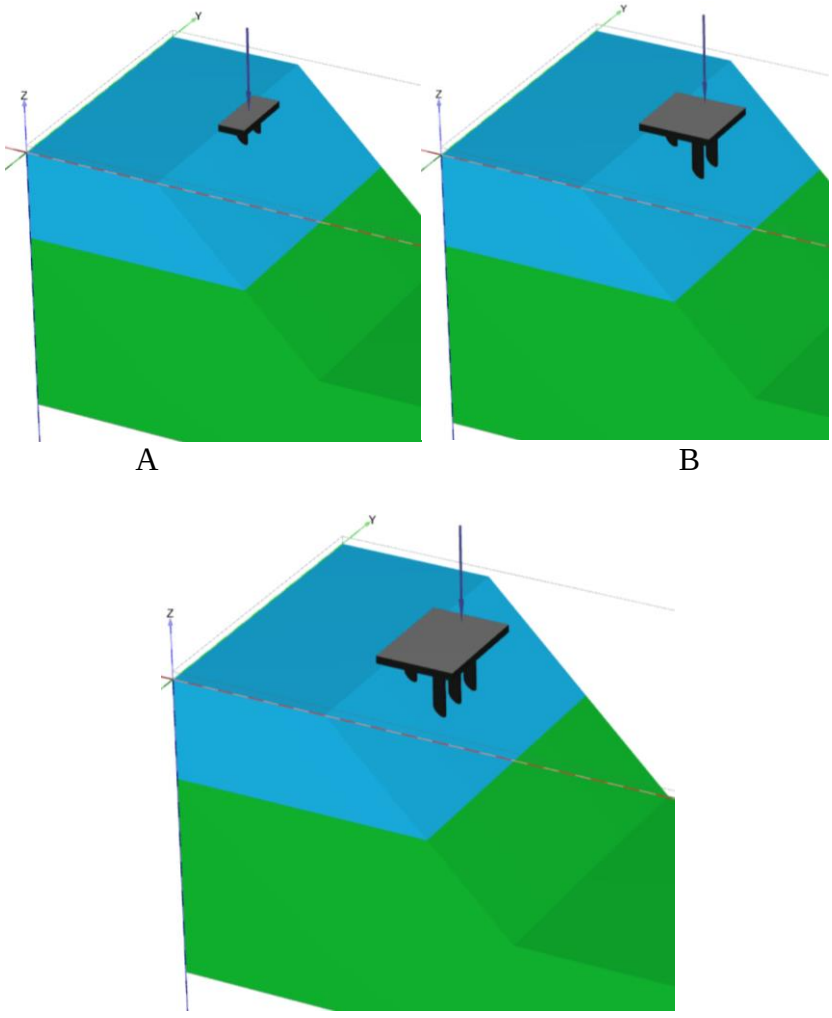

A B C

Figure 4. Model of pile group (A) 2×1, (B) 2×2, (C) 2×3.

2.3 Soil Simulation

The qualities of the soil utilized are shown in **Table 2**. The water table level uses about 40 m underground (empirical value). The earth was modeled after an elastic-ideal plastic substance by employing the Mohr-Coulomb failure standard. The slant of internal friction (Ø) was measured as an empirical equation **(Hatanaka and Uchida, 1996)**. The slope was

1:1, and this slope simulates the gradient in Iraq. It was represented by the finite element software (Plaxis 3D Foundation 2020) **(Albusoda, 2016).**

Table 2. Soil properties **(Albusoda, 2016)**.

Soil properties	Clay	Sand
Modulus of elasticity (kN/m^2)	9000	19000
Poisson's ratio μ	0.4	0.3
The angle of internal friction Ø	-	38
Cohesion (kPa)	40	2
Unit weight γ_t (kN/m^3)	18.5	18

2.4 Numerical Simulation Around the Problem

PLAXIS 3D was utilized in the computer simulations of the issue at hand. The numerical analysis is carried out on a rectangular region measuring 80 × 20 m. Phases that are both consistent and subject to change were used. During the investigation, phases that are both were taken into consideration.

In the same way as before, the boundary constraints for the static analysis stage were applied. As was found in the prior studies, the bottom of the geometry was immobile in all directions to account for the impact of the rock stratum, while the left and right sides of the model could only move vertically. This was done to account for the fact that the bottom of the mesh was locked against movement in all directions. In addition, the viscous limits have been considered in the dynamic analysis stage to eliminate the effect of the wave reflected in the finite element model during the time-history finite element analysis. The viscous limits in question are $X_{max.}$ and $X_{min.}$ in the form of viscose, in addition to the other forms, Y and Z, have been fixed **(Fattah et al., 2015; Kholdebarin, 2016)**. The model's left and right sides now have one of these viscous boundaries attached to them.

Because it is anticipated that the rock layer will be placed at a depth of 19.5 m below the earth's natural surface, the numerical model's profundity has been set to 19.5 m. The length of the model is estimated to be 80 m, and its width is estimated to be 20 m, according to the calculations. The influence of the length of the finite element model was evaluated parametrically, and the results were used to determine its size. First, simulating various model lengths has completed the parametric analyses and then selecting one of those lengths. Once this length has been chosen, the analysis results will not be affected by the extension of the finite element model. It is essential to be aware that the results were attained by applying the Mohr-Coulomb model to sandy soil with a relative density of about 50% and clay soil with a cohesiveness of 40 kPa. This information was used in the study.

The mesh size is medium. Seismic loading that was derived from the Halabjah, El-Centro, and Kobe earthquakes—each of which had peak accelerations of 0.10 g, 0.35 g, and 0.58 g, respectively—was utilized to model the foundation reaction, as can be seen in **Figs. 5 to 7.** This method is typical for modeling the earthquake's effect using finite element analysis. The seismic event is replicated by the use of this approach, wherein it is represented as a predetermined acceleration that is imposed on the lower portion of the finite element model, namely at the position corresponding to the rock layer **(Kholdebarin, 2016; Dhar, 2019).** The linear elastic model is used to simulate the pile foundation reaction. In this simulation, the E and values of the concrete foundation are assumed to be 30 GPa and 0.15, respectively.

These assumptions are in line with earlier research **(Alzabeebee, 2020).** During the static phase, a static point load was applied to the pile to simulate the pressure the residential building would apply. It was determined that the maximum point load that could be used for a single pile is 1265 kN.

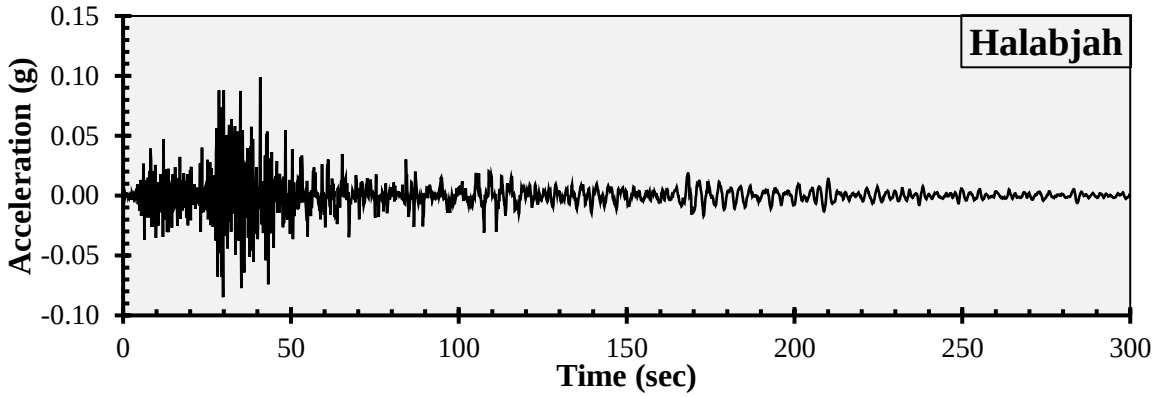

Figure 5. The Halabjah earthquake set a record for the acceleration duration.

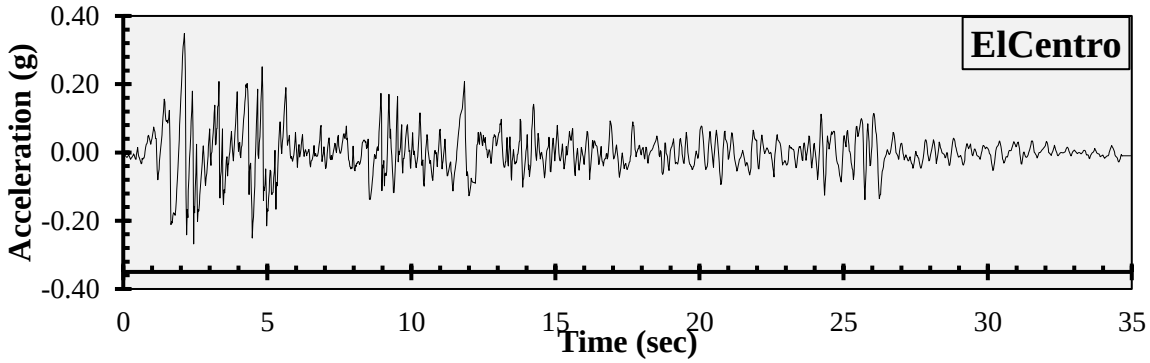

Figure 6. The El-Centro earthquake set a record for the acceleration duration.

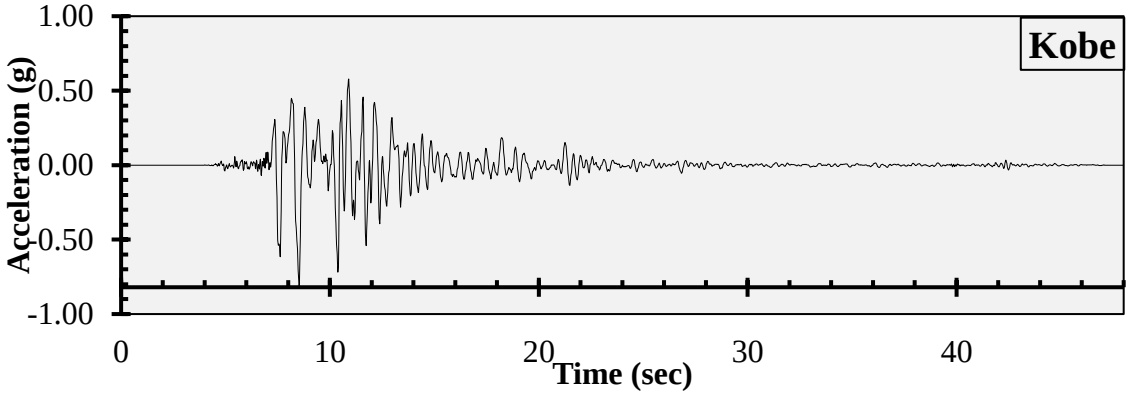

Figure 7. The Kobe earthquake set a record for the acceleration duration.

The three stages of analysis that were performed on the model created are:

- Determining the pressures at the beginning of the process placed on the soil is the focus of the first phase of the process. The soil density and the ground pressure damping factor played essential roles in the calculations. To determine these initial stresses.
- The second phase involves applying the point load to the pile as the final step in the process (which is 1265 kN, as mentioned previously).

- The discrete element method of time series analysis was used. To be carried out as part of the third phase of the project. This remained accomplished by triggering the model's viscose limitations and the earthquake located at the base of the model.

3. RESULTS AND DISCUSSION

Per examining numerous factors, this study reveals the effect of slopes on the pil. The following parameters are used:

- Slope: 1H:1V
- The ratio of length to diameter: L/D = 20
- Pile diameter (D) and pile length (L): D = 0.75 m, L = 15 m

3.1 Determination of The allowable Load on The Single Pile

According to (**Terzaghi, 1943),** a failure is known as a necessary load to displace 10% of the pile's diameter, the failure load is equal to 1897 kN, and a safety factor is relied on equal to 1.5. The allowable load is determined (1265 kN) based on that. The settlement is calculated at the node at the top of the pile, as shown in the results in **Fig. 8**.

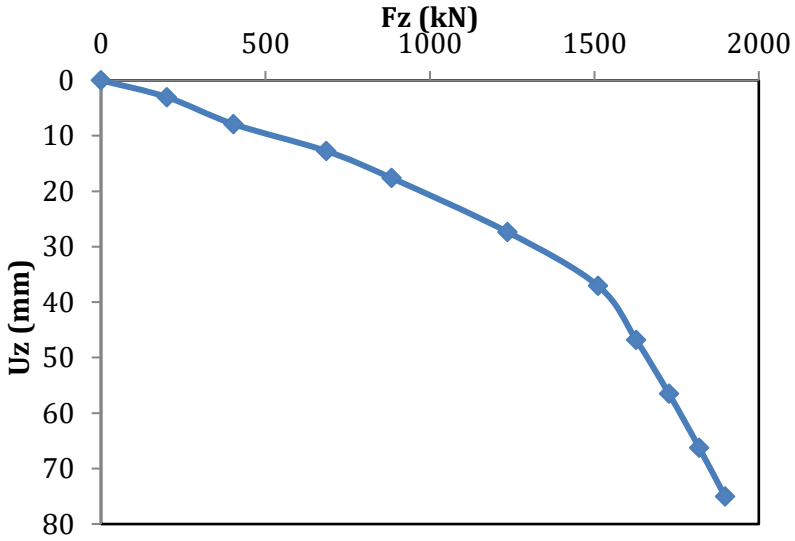

Figure 8. The load-settlement curve of the single pile, L=15 m, D=0.75 m.

The apparent settlement due to static load is given in **Table 3.**

Table 3. Settlement of pile group due to static load.

A pattern of pile group	Settlement (mm)
2×1	30
2×2	28
2×3	41

3.2 The Effect of Earthquakes on the Pattern of Pile Group

3.2.1 The effect of earthquakes on the settlement with 2×1 pile group

The study found that the influence of earthquakes (A=0.1 g, 0.35 g, and 0.58 g) on slope 1:1 pile group settlement increased the settlement about what it was in the vertical load only. **Fig. 9** shows the influence of the increase in settlement during earthquakes. The values of additional settlement resulting from the different earthquakes were equal to 4, 8, and 18 mm, respectively.

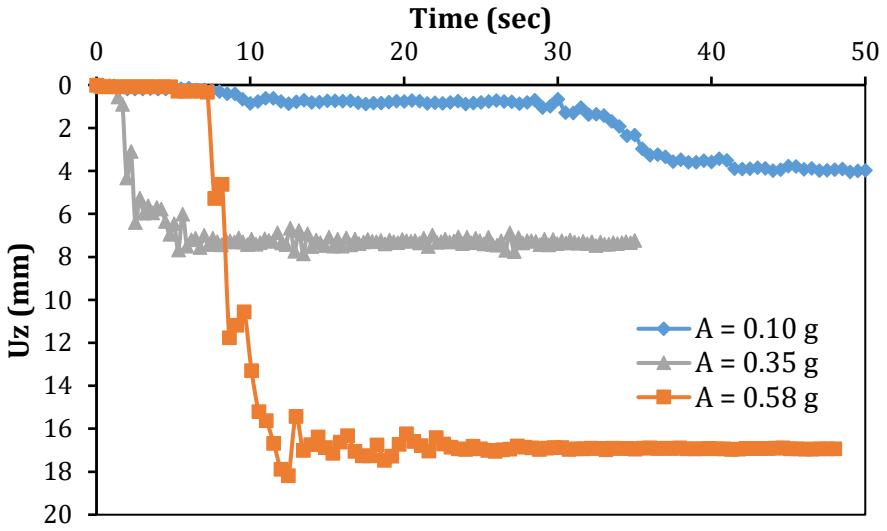

Figure 9. Time-settlement curve during earthquakes with 2×1 pile group.

3.2.2 The effect of earthquakes on the settlement with 2×2 pile group

The study found that the influence of earthquakes (A=0.1 g, 0.35 g, and 0.58 g) on slope 1:1 pile group settlement increased the settlement about what it was in the vertical load only. **Fig. 10** reported the influence of the increase in settlement during earthquakes.

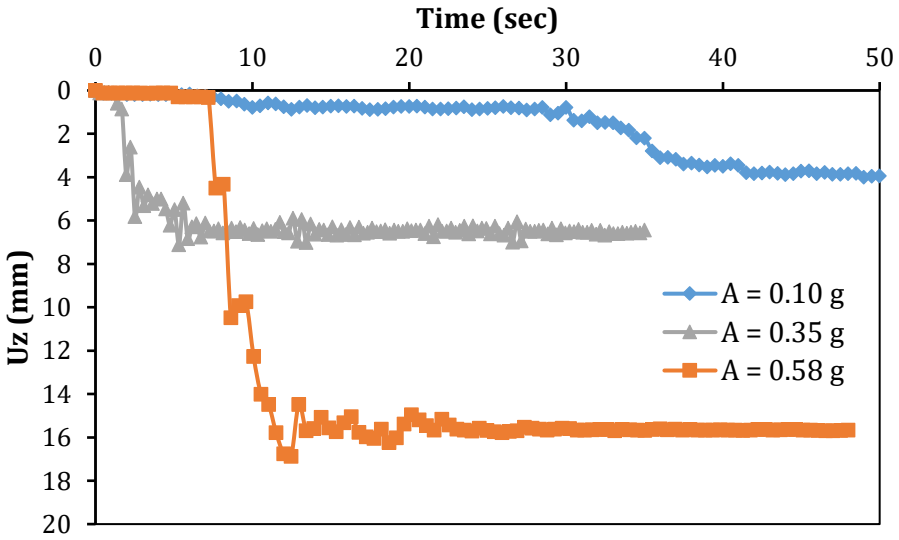

Figure 10. Time-settlement curve during earthquakes with 2×2 pile group.

Fig. 10 shows the values of additional settlement resulting from the different earthquakes were equal to 4, 7, and 17 mm, respectively.

3.2.3 The effect of earthquakes on the settlement with 2×3 pile group

The study found that the influence of earthquakes (A=0.1 g, 0.35 g, and 0.58 g) on slope 1:1 pile group settlement increased the settlement about what it was in the vertical load only. **Fig. 11** shows the influence of the increase in settlement during earthquakes. The amount added to the allowable settlement equals 4, 8, and 19 mm, respectively.

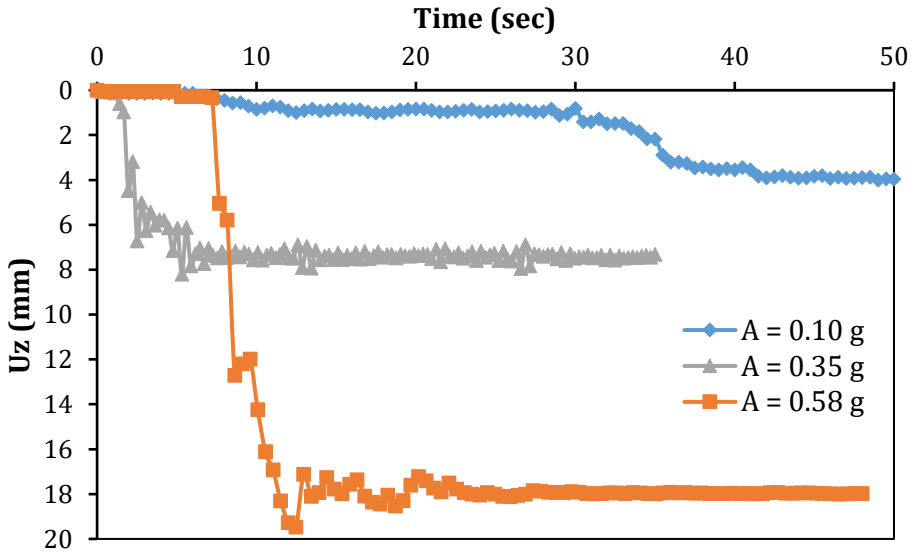

Figure 11. Time-settlement curve during earthquakes with 2×3 pile group.

Summary of the obtained results of the present work are given in **Table 4** and shown in **Fig. 12**.

Table 4. Settlement values for each earthquake.

The pattern of pile group	Settlement due to static load (mm)	Type of earthquake	Settlement due to dynamic load (mm)	Total settlement (mm)
2×1	30	Halabjah	4	34
		El-Centro	8	38
		Kobe	18	48
2×2	28	Halabjah	4	32
		El-Centro	7	35
		Kobe	17	45
2×3	41	Halabjah	4	45
		El-Centro	8	49
		Kobe	19	60

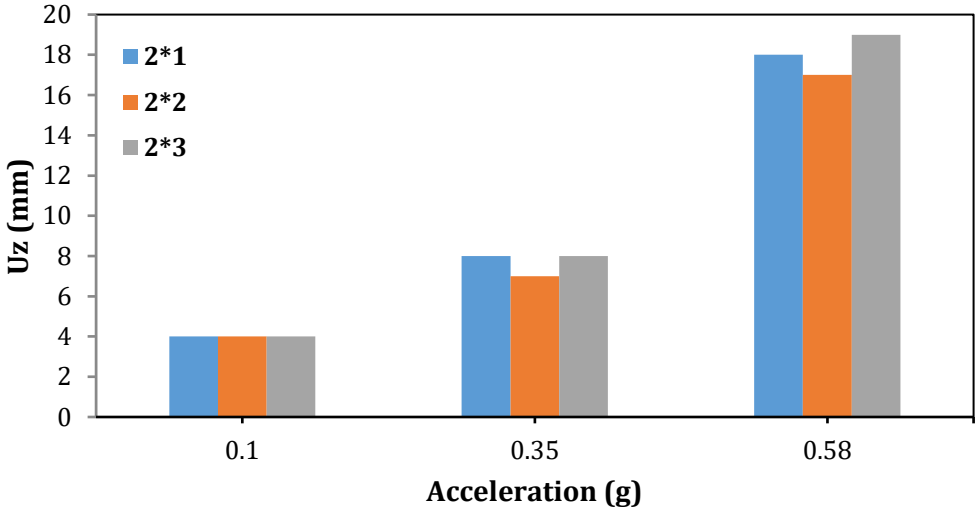

Figure 12. Settlement of different pile groups during earthquakes.

4. CONCLUSIONS

Different methods are used with Baghdad soil parameters in Plaxis 3D, and we used earthquakes of different acceleration to study settlement in more than one case. Here's a quick summary of what we learned:

- With the results obtained in this study, the vertical load leads to a very small horizontal displacement, which is hardly negligible due to the lateral earth pressure.
- It is observed that the acceleration in the earthquake of the waves significantly impacts the values of settlement.
- It has been observed that there is a difference in the results between the different earthquakes, and they do not have a fixed behavior due to the difference in acceleration and the difference in the period.
- The lowest settlement values for all models (2×1, 2×2, and 2×3) were recorded during the Halabjah earthquake 4.44, 4.60, and 4.13 mm.
- The largest settlement values for all models (2×1, 2×2, and 2×3) were recorded during the Kobe earthquake 18, 17, and 19 mm.

NOMENCLATURE

Symbol	Description	Symbol	Description
D	Diameter, m	N_{60}	SPT N-value corrected for field procedures only.
C	Cohesion, kPa		
E	Modulus of elasticity, MPa	Ø	The angle of internal friction, deg.
F	Load, N	γ_t	Unit weight, kN/m^3
L	Length, m	μ	Poisson's ratio, dimensionless

REFERENCES

Amer, A.N., Sobaih, M. and Adel, A., 2016. Investigation of effects of capacity spectrum method on performance evaluation of multi-story buildings according to the IRAQI seismic code requirements. *Open Journal of Civil Engineering*, 6(3), pp. 420-441.

Albusoda, B.S., 2016. Engineering assessments of liquefaction potential of Baghdad soil under dynamic loading. *Journal of Engineering and Sustainable Development*, 20(1), pp. 59-76.

Al-Mosawe, M.J., Al-Shakarchi, Y.J., and Al-Taie, S.M., 2007. Embedded in sandy soils with cavities. *Journal of Engineering*, 13(1), pp. 1168–1187.

Al-Taie, S.M., 2004. *The performance of laterally loaded piles embedded in sandy soils which contains cavities*. Master Thesis, Department of Civil Engineering, University of Baghdad. Iraq.

Alzabeebee, S., 2020. Dynamic response and design of a skirted strip foundation subjected to vertical vibration, *Geomech Engineering*, 20 (4), pp. 345-358. Doi:10.12989/gae.2020.20.4.345.

Arosemena, R.L., 2007. *Effect of horizontal piles on the soil bearing capacity for circular footing above cavity*. Electronic Theses and Dissertations. 3067, University of Central Florida, Orlando, Florida

Ben, Z., 2013. Large-scale finite element simulation of seismic soil-pile foundation-structure interaction. Doctoral thesis, National University of Singapore

Ben, Z., 2013. *Large-scale finite element simulation of seismic soil-pile foundation-structure interaction* (Doctoral dissertation).

Bowles, L.E., 1988. *Foundation analysis and design*. McGraw-hill. New York St. Louis San Francisco

Dhar, S., Ozcebe, A.G., Dasgupta, K., Petrini, L., and Paolucci, R., 2019. Different approaches for numerical modeling of seismic soil-structure interaction: impacts on the seismic response of a simplified reinforced concrete integral bridge. *Earthquakes and Structure,* 17(4), pp. 373-385. Doi:10.12989/eas.2019.17.4.373.

Fattah, M.Y., Zabar, B.S., and Mustafa, F.S., 2020. Effect of saturation on response of a single pile embedded in saturated sandy soil to vertical vibration. *European Journal of Environmental and Civil Engineering*, *24*(3), pp. 381–400.

Fattah, M.Y., Hamoo, M.J., and Dawood, S.H., 2015. Dynamic response of a lined tunnel with transmitting boundaries. *Earthquakes and Structure*, 8(1), pp. 275-304. Doi:10.12989/eas.2015.8.1.275.

Fellenius, B.H., 2009. *Basics of foundation design, a textbook*. Revised Electronic Edition, [WWW. Fellenius. Net], 330.

Fredlund, D.G., and Krahn, J., 1977. Comparison of slope stability methods of analysis. *Canadian Geotechnical Journal*, 14(3). Doi.10.1139/t77-045.

Fukuoka, M., 1977. The effects of horizontal loads on piles due to landslides. In Proceedings of the Specialty Session 10, the 9th International Conference on Soil Mechanics and Foundation Engineering, Tokyo, The Japanese Society of Soil Mechanics and Foundation Engineering, Tokyo, pp. 27–42

Griffiths, D.V., and Marquez, R.M., 2007. Three-dimensional slope stability analysis by elasto-plastic finite elements. *Geotechnique*, 57(6), pp. 537-546. Doi:10.1680/geot.2007.57.6.537.

Hatanaka, M., and Uchida, A., 1996. Empirical correlation between penetration resistance and internal friction angle of sandy soils. *Soils And Foundations,* 36 (4), pp. 1-9. Doi:10.3208/sandf.36.4_1

Ho, I., 2014. Numerical study of slope-stabilizing piles in undrained clayey slopes with a weak thin layer. *International Journal of Geomechanics*, 15 (5). Doi:10.1061/(ASCE)GM.1943-5622.0000445.

Huang, M., Wang, H., Sheng, D., and Liu, Y., 2013. Rotational translational mechanism for the upper bound stability analysis of slopes with weak interlayer. *Computers and Geotechnics*, 53, pp. 133-141. Doi:10.1016/j.compgeo.2013.05.007.

Ito, T., and Matsui, T., 1975. Methods to Estimate Lateral Force Acting on Stabilizing Piles, *Soils and Foundations,* 15 (4), pp 43-59. Doi:10.3208/sandf1972.15.4_43

Kholdebarin, A., Massumi, A., and Davoodi, M., 2016. Seismic bearing capacity of shallow footings on cement-improved soils. *Earthquakes and Structure,* 10(1), pp. 179-190. Doi:10.12989/eas.2016.10.1.179.

Lee, C.Y., Poulos, H.G., and Hull, T.S., 1991. Effect of seafloor instability on offshore pile foundations. *Canadian Geotechnical Journal*, 28(5), pp. 729-737. Doi:10.1139/t91-087.

Ling, H.I., and Leshchinsky, D., 1998. Effects of vertical acceleration on seismic design of geosynthetic-reinforced soil structures. *Geotechnique*, 48(3), pp. 347-373. Doi:10.1680/geot.1998.48.3.347

Ling, H.I., Leshchinsky, D., and Perry, E.B., 1997. Seismic design and performance of geosynthetic-reinforced soil structures. *Geotechnique*, 47(5), pp. 933-952. Doi:10.1680/geot.1997.47.5.933.

Liu, Z., Bishop, J.A. and Lindsey, J.K., 2016. Study of combined pile raft foundations for heavy dynamic equipment. In *Geotechnical and Structural Engineering Congress 2016,* pp. 829-840.

Michalowski, R.L., 2007. Displacements of multiblock geotechnical structures subjected to seismic excitation. *Journal of Geotechnical and Geoenvironmental Engineering*, 133(11) Doi:10.1061/(ASCE)1090-0241(2007)133:11(1432)

Newmark, N.M., 1965. Effects of earthquakes on dams and embankments. *Geotechnique*, 15(2), pp. 139–160. Doi:10.1680/geot.1965.15.2.139.

Novak, M., 1974. Dynamic stiffness and damping of piles. *Canadian Geotechnical Journal*, *11*(4), pp. 574–598

Novak, M., and Grigg, F.R., 1976. Dynamic experiments with small pile foundations. Canadian Geotechnical Journal, 13(4), pp. 372–385.

Proceedings of speciality session 10, ninth international conference on soil mechanics and foundation engineering, Tokyo, July 1977, pp. 27-42. (in French)

Reese, L.C., Isenhower, W.M. and Wang, S.T., 2005. *Analysis and design of shallow and deep foundations* (Vol. 10). John Wiley & Sons.

Seed, H.B., Lee, K.L., and Idriss, I.M., 1969. Analysis of the Sheffield dam failure," *Journal of the Soil Mechanics and Foundations Division*. ASCE, 95(6), Doi:10.1061/JSFEAQ.0001352.

Shlash, K.T., Mahmoud, M.R. and Aziz, L.J., 2012. Lateral resistance of a single pile embedded in sand with cavities. *Eng. & Tech. Journal*, *30*(15), pp. 2641-2663.

Sowers, G.F., 1996, June. Building on sinkholes: design and construction of foundations in karst terrain. American Society of Civil Engineers.

Terzaghi, K., 1943, *Theoretical Soil Mechanics*. John Wiley & Sons, New York.

Viggiani, C., 1981. Ultimate lateral load on piles used to stabilize landslides. 10th International Conference on Soil Mechanics and Foundation Engineering (Stockholm), Sweden, pp. 555-560.